

MOLECULAR DYNAMICS SIMULATION OF COPOLYMERS

MICHAŁ BANASZAK

*Macromolecular Physics Laboratory,
Institute of Physics, A. Mickiewicz University,
Umultowska 85, 61-614 Poznan, Poland
mbanasz@amu.edu.pl*

(Received 28 November 2000)

Abstract: A series of representative Molecular Dynamics simulations of model Lennard-Jones copolymer chains is presented. We report measurements of thermodynamic, structural and dynamic properties of our model copolymers. For neutral copolymers we confirm our version of Thermodynamic Perturbation Theory of the First Order, while for ionic copolymers we demonstrate microphase formation and the anisotropy of the counterion diffusion.

Keywords: molecular dynamics, computer simulation, copolymer, diblock, ionic copolymer, diffusion, structure factor, equation of state, thermodynamic properties

1. Introduction

Copolymers are polymers composed of different types of monomers. Thermodynamic properties of copolymers are relatively insensitive to monomer distribution along the polymer chain, but the structural and dynamic properties depend on it in a significant way. Copolymer phase behaviour and mesoscopic behaviour are also heavily influenced by the monomer distributions along the chain. Usually copolymers are described as either random, alternating and block copolymers, with further subdivision of block copolymers into diblock copolymers (in case of 2 blocks) and triblocks (in case of 3 blocks). The goal of this paper is to present a selected set of Molecular Dynamics (MD) computer simulations on miscellaneous model copolymer systems in order to show some new results and challenges in this appealing field. In particular, our objective is to show thermodynamic, structural and dynamic properties of those systems. The easiest to measure are thermodynamic properties due to the relatively short relaxation times, and thus rapid equilibration. The structural and dynamic properties, on the other hand, are more difficult to obtain because of the long corresponding relaxation times, and thus sluggish equilibration.

Theoretical equations of state (EOS) for model chain molecules, usually composed of freely-jointed tangent segments interacting via a spherically symmetric potential, are commonly used as prototypes for the engineering EOS models of real polymer systems [1–18].

These equations of state are often used to calculate the phase equilibria of real polymer systems.

Banaszak *et al.* [19] developed a formalism, based on Wertheim's thermodynamic perturbation theory of the first order (TPT1), to calculate EOS of copolymer chains. It was also demonstrated that this formalism successfully predicts the phase equilibria for real copolymer solution [15]. In this formalism [1, 19] the thermodynamic properties of the polymer fluid are calculated from the thermodynamic and structural properties of the segment fluid, also referred to as the reference fluid. As a reference fluid for our model we chose a fluid composed of Lennard-Jones (LJ) spheres, *i.e.*, point particles interacting with the LJ model potential. In order to use TPT1 to calculate the Helmholtz energy (and other thermodynamic quantities, such as pressure and chemical potentials) of polymer mixtures consisting of LJ segments, one needs to know the properties of the LJ reference fluid. These properties can be obtained analytically by using different mixing rules as shown by Banaszak *et al.* [6]. In this paper we show MD simulations of neutral, that is without electric charges, copolymer LJ chain. Those simulations are to confirm our implementation of TPT1.

Apart from neutral copolymers we have simulated ionic copolymers, that is copolymers carrying electric charges. Ionic polymers (polyelectrolytes, ionomers) are of considerable current interest [20, 21]. In those systems one ionic species, *e.g.*, anion, is chemically bonded to the polymer chain either to a pendant group or to the backbone chain; the cation (counterion), on the other hand, is not chemically bonded to the chain and free to move if its thermal energy can overcome the electrostatic forces.

It should be noted that while ionic polymer dilute solutions are fairly well understood, this is not the case for ionic polymer melts. We expect, however, a great deal of both excluded volume interaction screening and electrostatic interaction screening [22].

Since the counterion transport properties in microphase-separated ionic copolymers are of great practical interest, we want to probe the relationship between counterion diffusion and microstructure. Finally by gaining insight into the symmetric diblock case, we lay foundations for our future studies, *i.e.*, simulations of asymmetric ionic diblocks, ionic multiblocks or ionic branched copolymers such as NAFION, or lipid bilayers.

Neutral diblock copolymers can self-assemble into a variety of ordered microstructures. This self-assembly or ordering takes place as those copolymers are cooled down from a disordered high temperature phase to low temperature ordered phase. This process is called order-disorder transition (ODT) or also microphase separation transition (MST), and is characterized by a temperature which marks the onset of long range order T_{ODT} . It is well established experimentally that the microphase (ordered phase) can look like an array of bcc spheres, hexagonally packed cylinders, or spatially ordered layers. These microphases are often referred to as the "classical" microstructures. Close to the ODT the interface between the microdomains is diffused, and interfaces can fill up most of the space. This segregation regime is called weak segregation limit (WSL). By contrast, when the interfaces between microdomains are sharp and highly localized the system is in strong segregation limit (SSL). The diblock copolymer microstructure in the strong segregation regime is largely determined by volumetric considerations. The diblocks with roughly the same volume of both species form layers (lamellae), while diblock with significant (more

than about 80% by volume) excess of one species form ordered spheres (micelles). The diblocks with intermediate volume fractions usually form hexagonally packed cylinders. Apart from those ‘classical’ microstructures, there have been discovered ‘non-classical’ bicontinuous microstructures such as ordered bicontinuous double diamond (OBDD) structure ($Pn\bar{3}m$ space group), gyroid bicontinuous structure ($Ia\bar{3}d$ space group) and hexagonally perforated layers. There is still some controversy about the existence and thermodynamic stability of those ‘non-classical’ microstructures. The experimental phase diagram of a real diblock copolymer can be found in, *e.g.*, reference [23].

For ionic copolymer simulations the reduced density, $\rho^* = \sigma^3 \rho$ (where σ is the diameter of the bead), is initially set to 0.5 which is closer to the semidilute regime than to a melt. This low bead density was chosen in order to speed up the equilibration. Our model system consists of twenty 31-mer diblocks and 160 cations, total 780 atoms, confined in a cubic box yielding the desired density. However, some simulations were carried out using 160 chains and 1280 cations. It was necessary to restrict the chain lengths due to the very slow structural relaxation times in these systems.

2. Model

In our model each chain is a sequence of connected LJ segments. The Lennard-Jones interaction potential between the segment is:

$$V_{\alpha\beta}(r) = 4\varepsilon_{\alpha\beta} \left(\left(\frac{\sigma}{r} \right)^{12} - \left(\frac{\sigma}{r} \right)^6 \right)$$

with the minimum of the potential at

$$r_0 = (2)^{\frac{1}{6}} \sigma,$$

$\alpha, \beta = 1$ or 2 , and the depth of the potential between segments α, β is $\varepsilon_{\alpha\beta}$. We allow for both intermolecular and intramolecular interactions except for nearest-neighbors along the chain.

First we consider two model cases of neutral LJ chains. In the first case, we consider a mixture of two types of homonuclear chains, one composed of segments of type 1 and the other of segments of type 2, which can be thought of as a homopolymer blend (Figure 1). Next we consider a pure-component fluid containing neutral LJ copolymer chains, composed of segments of type 1 and 2, which can be thought of as a copolymer melt (Figure 2), either block copolymer (2a), or blocky copolymer (2b) or alternating copolymer (2c). The compressibility factor, $Z = P/(\rho T)$ (where P is pressure, ρ number density, and T temperature), for these two cases is calculated using the general theory developed by Banaszak *et al.* [19].

Our ionic diblock copolymer, shown schematically in Figure 3, consists of a neutral block of 15 beads, and the ionic block of 16 beads; in the latter block every second bead carries a negative elementary charge. Eight positively charged beads, *i.e.*, cations, are included to maintain electroneutrality. Volumetrically this makes the system slightly asymmetric in favor of ionic block.

In this case we have used a simplified LJ interaction potential which incorporates explicit electrostatic contributions superimposed on universal excluded volume interactions. Long range ion interactions are calculated by the Ewald method. The excluded volume effect is modelled using the purely repulsive ‘‘WCA’’ modification of the Lennard-Jones (LJ)

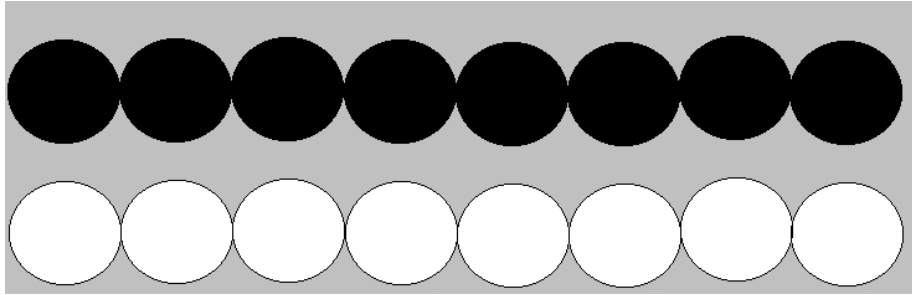


Figure 1. Binary homopolymer melt; segments of type 1 white and segments of type 2 black

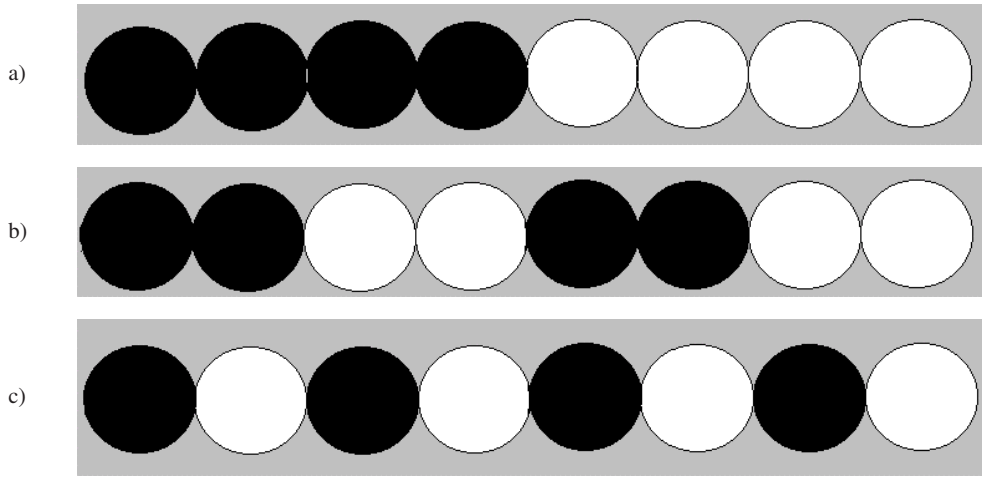


Figure 2. a) Block copolymer melt; b) blocky copolymer melt; c) alternating copolymer melt

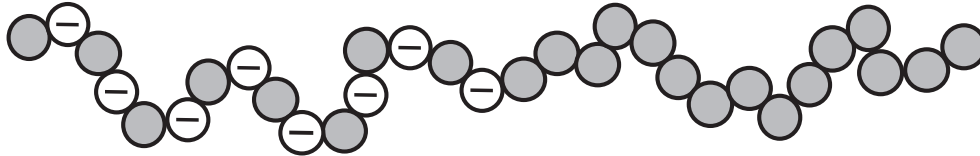


Figure 3. Schematic picture of the ionic copolymer chain

potential between interactions centres representing neutral monomers, anionic monomers and “free” cations:

$$\begin{aligned} \phi_{\text{WCA}}(r_{ij}) &= 4\epsilon((\sigma/r_{ij})^{12} - (\sigma/r_{ij})^6) + \epsilon \quad \text{for } r_{ij} \leq 2^{1/6}\sigma, \\ \phi_{\text{WCA}}(r_{ij}) &= 0 \quad \text{for } r_{ij} > 2^{1/6}\sigma. \end{aligned}$$

Here r_{ij} is the separation of monomers i and j , ϵ and σ are the usual LJ parameters which have the same magnitude for all beads. The link length between beads was set equal to σ .

Including coulomb interactions between the charges the total interaction potential can therefore be written as follows:

$$\phi_{\text{TOTAL}}(r_{ij}) = \left(\frac{q_i q_j e^2}{4\pi \epsilon_0 \epsilon_R \sigma} \right) \left(\frac{\sigma}{r_{ij}} \right) + \phi_{\text{WCA}}(r_{ij}),$$

where the q 's are charge numbers and ϵ_R is the dielectric constant. We can write this in a more useful form:

$$\phi_{\text{TOTAL}}(r_{ij}) = E_{\sigma}^{ij} \frac{\sigma}{r_{ij}} + \phi_{\text{WCA}}(r_{ij}),$$

where E_{σ}^{ij} is the electrostatic potential at an ion separation of σ . Since the unlike charge interaction provides the only cohesive energy in the model we define E_{σ} as a measure of the depth of this potential where $E_{\sigma} = |E_{\sigma}^{\pm}|$.

For a given value of σ temperature is thus reported as $T^* = kT/E_{\sigma}$, density as $\rho^* = N\sigma^3/V$, pressure as $P^* = P\sigma^3/E_{\sigma}$, and time as $t^* = t(E_{\sigma}/(m\sigma^2))^{1/2}$, where m is the mass of the bead. The optimized time step Δt^* was found to be 0.044.

In our simulations we measured those properties which are the most useful in determining the ODT and the characterization of cation transport properties. First of all we measured the partial structure factors, defined as follows:

$$S_{\alpha\alpha}(\vec{k}) = \frac{1}{N} \left\langle \left[\sum_{i=1}^{N_{\alpha}} (\sin \vec{k}_i \vec{r}_i) \right]^2 + \left[\sum_{i=1}^{N_{\alpha}} (\cos \vec{k}_i \vec{r}_i) \right]^2 \right\rangle_{\text{thermal average}}$$

where N is the total number of atoms, and N_{α} is the number of atoms of type α , for example cations, and the summation over label i runs through all the atoms of type α . In disordered isotropic phase the structure factor can be spherically averaged since all spatial directions are equivalent:

$$S_{\alpha\alpha}(k) = \left\langle S_{\alpha\alpha}(\vec{k}) \right\rangle_{\text{average over all directions}}$$

3. Simulation results

Since our main interest is in the universal properties of the neutral and ionic copolymers, we employ a coarse-grained (mesoscopic) model, that is Lennard-Jones potential and electrostatic potential. This means that we ignore the valence angle potential and the torsional potential, and keep only the rigid bonds along the chain, short range repulsive interaction and the electrostatic interactions.

The equations of motions for the model LJ chains are integrated using the Verlet algorithm and the bond length, set equal to σ , is kept constant using the SHAKE algorithm [24]. The temperature is controlled using a weak coupling to an external thermal bath [25]. In our simulations we use molecular dynamics with Berendsen loose coupling, either only to thermostat ('NVT'), or both to barostat and thermostat ('NPT').

For neutral LJ chains we have simulated using 'NVT' at selected densities. First a homopolymer blend at $T_{11}^* = T/\epsilon_{11} = 3.0$ and 6.0 and LJ potential with $\epsilon_{22}/\epsilon_{11} = 1.5$, $\sigma_{11}/\sigma_{22} = 1.0$, $m_1 = m_2 = 8$ and $x_1 = x_2 = 0.5$, where m_1 and m_2 are monomer numbers, while x_1 and x_2 are volume fractions of chain 1 and 2, respectively. Using our version of TPT1 [26] to determine the corresponding compressibility factor, Z , we notice that our TPT1 compressibility factors follow the MD data for both temperatures (Figures 4a and 4b).

Then we have simulated copolymer melts at $T_{11}^* = 2.0$ and 6.0, with LJ potential and 3 different microarchitectures (Figures 2a, 2b and 2c); $m = 8$, $\epsilon_{22}/\epsilon_{11} = 1.5$, $\sigma_{11}/\sigma_{22} = 1.0$, and $x_1 = x_2 = 0.5$. The MD compressibility factors for the selected densities are virtually the same for all 3 microarchitectures, which shows that for a given composition the EOS does not depend heavily on the linear copolymer monomer distribution. Moreover we notice

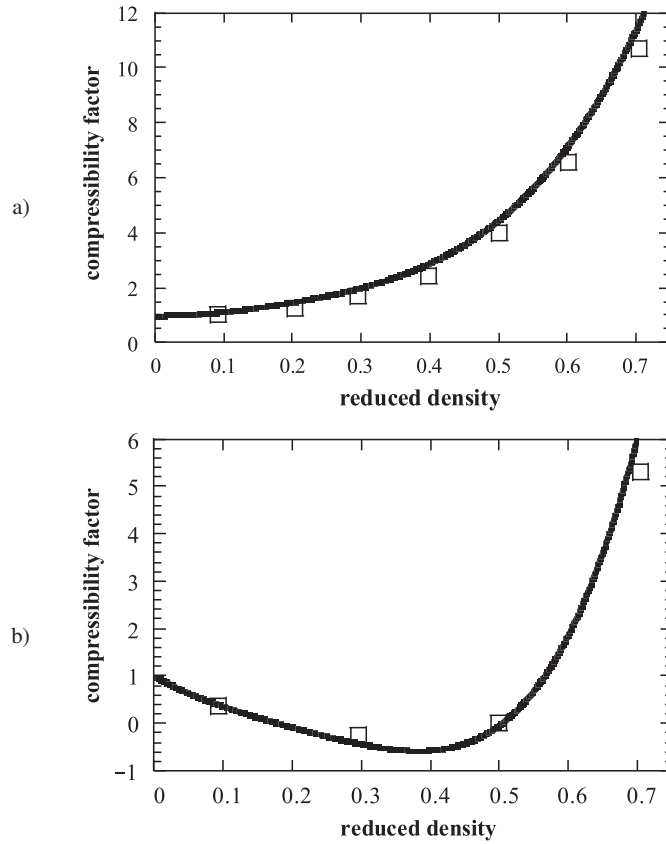


Figure 4. a) Compressibility factor for binary homopolymer blend $T_{11}^* = 6.0$, continuous line – TPT1 calculation, squares – simulation results; b) compressibility factor for binary homopolymer blend $T_{11}^* = 3.0$, continuous line – TPT1 calculation, squares – simulation results

that our TPT1 compressibility factors similarly follow the MD data for both temperatures (Figures 5a and 5b).

Now let us present our simulations for ionic copolymers. First we turn our attention to ‘NVT’ results. In Figure 6 we show the temperature dependence of four properties which clearly indicate the onset of microphase separation in the ionic copolymer. These results were obtained by cooling an $N = 20$ sample initially prepared as an isotropic disordered melt and equilibrated for 10^5 steps at $T^* = 0.096$ which is more than twice the temperature of the ODT. The cooling to $T^* = 0.024$ was accomplished incrementally in 14 stages; at each stage the system was equilibrated for 5×10^4 time steps followed by a sampling period of 5×10^4 steps.

At temperatures between 0.096 and ~ 0.04 the melt samples were homogeneous and the appearance of a strong nearest neighbour peak in the unlike charge radial distribution functions was clear evidence for the existence of counterion condensation on the ionic blocks. Visualization of sample structures revealed that below $T^* \sim 0.04$ the structure became anisotropic and a lamella morphology could be distinguished (see Figure 7) as would be predicted for a near symmetric block copolymer. In periodic systems the

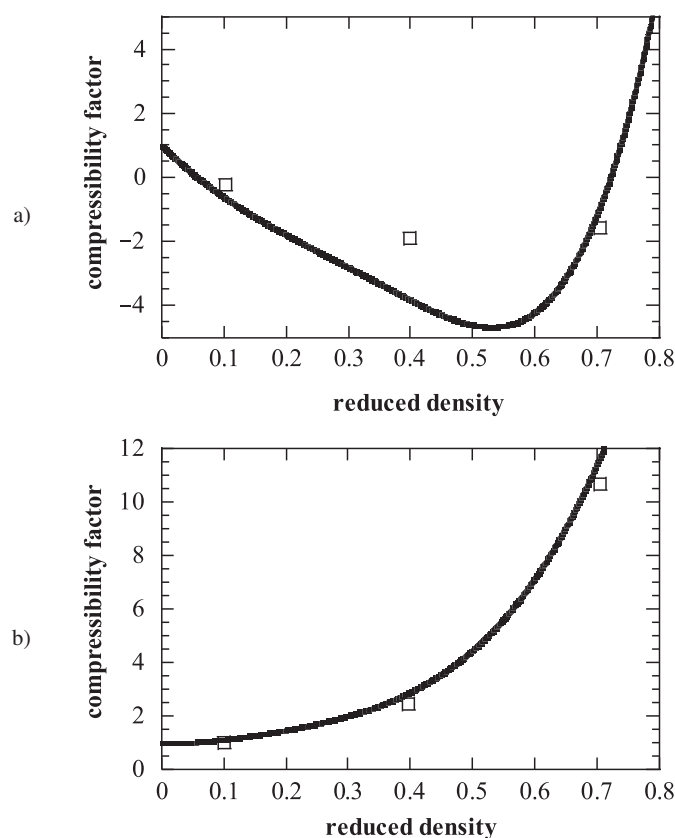


Figure 5. a) Compressibility factor for copolymer melt $T_{11}^* = 2.0$, continuous line – TPT1 calculation, squares – simulation results; b) Compressibility factor for copolymer melt $T_{11}^* = 6.0$, continuous line – TPT1 calculation, squares – simulation results

sample spontaneously adopts a layer structure which is commensurate with the periodic boundaries of the simulation cell. The negative and positive ion partial structure factors are indistinguishable for the ordered microphase and in our simulations the peaks in these structure factors show that the lamella periodicity for the $N = 20$ system is $L/2$ (11.6σ) and the symmetry of the system is broken in the 100 direction while for the $N = 160$ sample the periodicity is $L/\sqrt{2}$ (16.4σ), the broken symmetry being perpendicular to a 110 direction of the cubic cell.

The anisotropy of the structure factor [12] shows clearly the onset of structural order for wave vectors corresponding to the low-k peak in the structure factor. The principal moments of the angular distribution of structure factor, $S(\mathbf{k})$, are ordered such that $\lambda_1 \leq \lambda_2 \leq \lambda_3$. Symmetry breakdown accompanying ODT can then be characterized by two invariants, Q_1 and Q_2 . $Q_1 = \frac{\lambda_2 + \lambda_3}{\lambda_1} - 2$ and for lamella symmetry is predicted to be significantly different from zero. It is shown in Figure 6a that as the sample is cooled Q_1 gradually increases and starts to fluctuate. It then changes rapidly to a value of about 0.5, suggesting that the ODT at about $T^* = 0.043$. $Q_2 = \frac{\lambda_3 - \lambda_2}{\lambda_1}$ as expected remains close to zero.

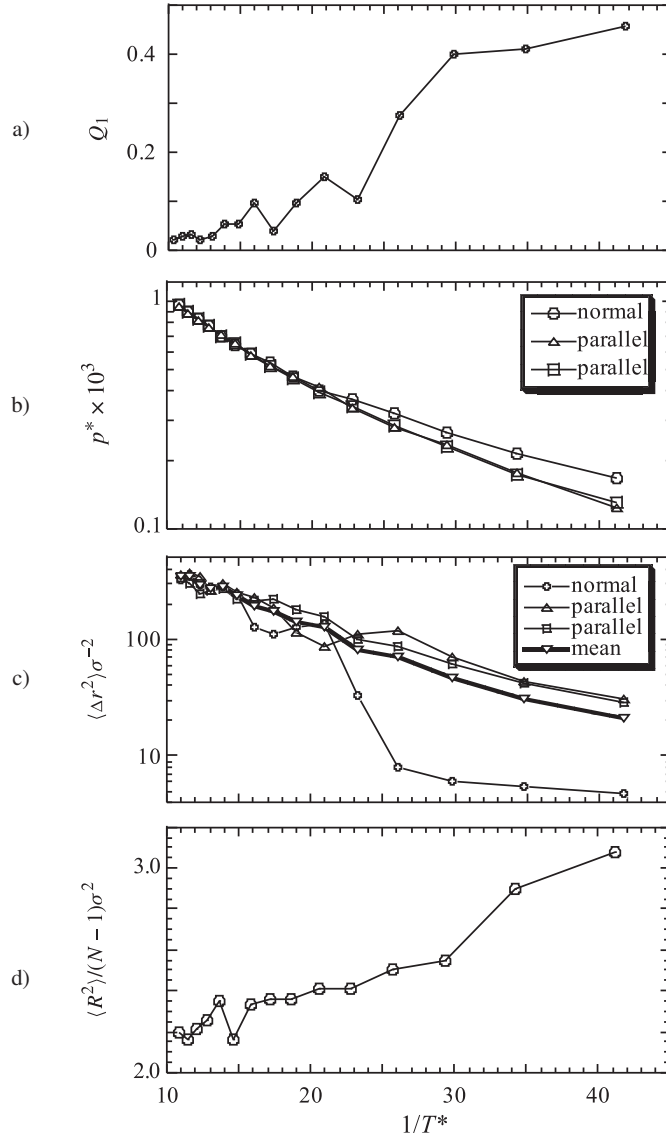


Figure 6. Inverse temperature dependence of properties showing the onset of microphase separation on cooling the smaller ($N=20$) sample: a) the anisotropy invariant Q_1 of the directional structure factor $S(\mathbf{k})$, evaluated for a spherical shell with $8 > kL/\pi > 2$; b) pressure components normal and tangential to eventual lamella plane of the microphase; c) mean squared displacements for counterions normal and tangential to eventual lamella plane of the microphase after 5×10^4 time steps; d) chain mean squared end-to-end distance, showing chain expansion through the ODT

At high temperature in the disordered phase the diagonal components of the pressure tensor, P_{xx} , P_{yy} and P_{zz} , are all equal within the statistical error (Figure 6b), but at about $T^* = 0.048$, the pressure in the direction of symmetry breakdown starts to increase due to the onset of lamella ordering. At $T^* = 0.024$ the sample is well into the microphase-separated region and there is a significant difference in the tensor components normal and parallel to the direction of lamellar ordering.

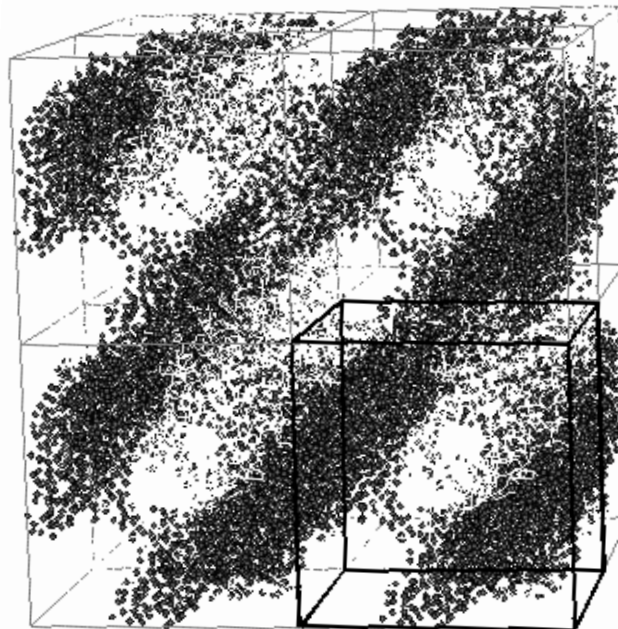


Figure 7. Instantaneous snapshot of the microphase structure in the 160 chain system at a temperature of $T^* = 0.024$; 8 neighbouring periodic cells are shown to emphasize the lamellar morphology

There is a significant increase of copolymer square end-to-end distance as the system is cooled through the ODT and the two dissimilar blocks become separated in space, as shown in Figure 6d.

A quantity of considerable interest in these ionic systems is the counterion diffusion constant, which is related to the ionic conductivity. As the system undergoes separation the counterions distribute themselves in the alternate ionic layers and consequently the counterion mobility in a direction normal to the layers decreases rapidly at the ODT as shown in Figure 6c. In the direction parallel to the lamella planes the diffusional mobility remains high over the whole temperature range studied.

Now we turn our attention to ‘NPT’ results. These results were obtained by cooling an $N = 20$ sample initially prepared as an isotropic disordered melt at high temperature. The cooling to $T^* = 0.024$ was accomplished incrementally in 14 stages; at each stage the system was equilibrated followed by a sampling period. As we cool the system, we monitored its properties. In particular, we looked at the square end-to-end distance of the polymer chains, which is expected to increase as we lower the temperature with more dramatic expansion in the vicinity of ODT. We also measured the square end-to-end distances for both blocks, neutral and charged. The results indicated an increase of copolymer square end-to-end distance as the system is cooled [27].

We also measured box dimensions and density, Figure 8 (a and b). At high-temperature disordered phase all diagonal components, L_x , L_y , L_z are equal within the statistical error, but at about $T^* = 0.07$ just before the ODT, the dimension in the direction of symmetry breakdown starts to increase, an indication of a force driving the ODT. At $T^* = 0.024$, which

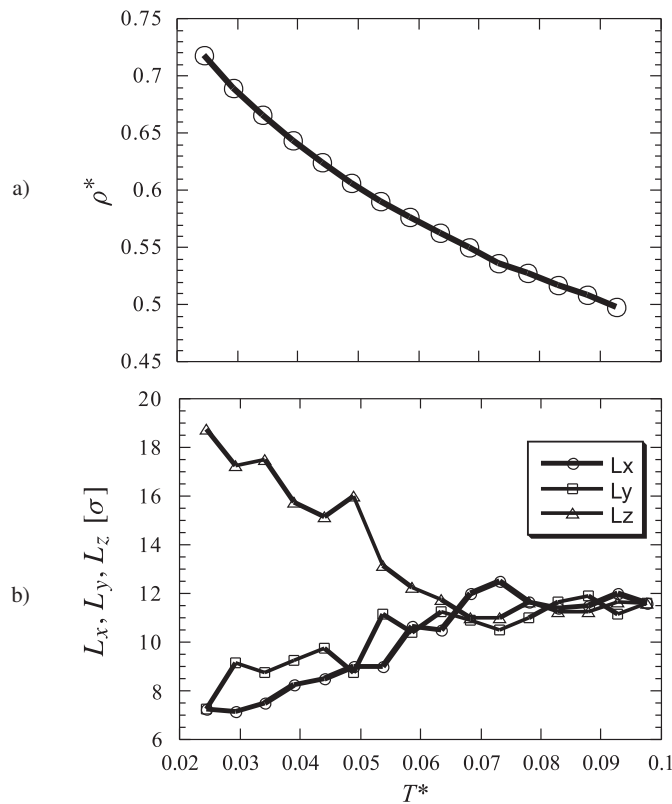


Figure 8. Temperature dependence for 2 properties in ‘NPT’ cooling: a) density; b) box dimensions

is well microphase-separated, there is a significant difference in box dimensions. Similarly the density is increased as the system is cooled.

4. Conclusion

We have tested our extension of TPT1 to heterobonded LJ chains by performing an MD simulation on a set of model LJ chains. The results indicate that this version of TPT1 can be used in phase equilibria predictions for copolymer solutions, as we have already demonstrated elsewhere [19]. We also notice that both the simulation data and the corresponding TPT1 predictions do not discriminate between different linear copolymer monomer distributions (block, blocky, alternating). Further simulations and the refinement of TPT1 are underway. We have also presented a generic coarse-grain (mesoscopic) model for simulation studies which can be used effectively to study selforganization in ionic copolymers. Ion condensation screens the intensity and range of the electrostatic interactions and for the near symmetric block copolymer studied here this leads to microphase separation which has very similar characteristics to that observed in purely neutral copolymers. It also results in decoupled diffusion of counterions. The dimensions of the microphase in the ‘NVT’ cooling are distorted by boundary conditions but such effects were reduced by using controlled pressure ‘NPT’ cooling.

Acknowledgements

Partial support by the Polish Committee for Scientific Research (KBN) project 8T11F 01214 is acknowledged.

References

- [1] Wertheim M S 1986 *J. Chem. Phys.* **87** 7323
- [2] Chapman W G, Gubbins K E, Jackson G and Radosz M 1990 *Ind. Eng. Chem. Res.* **29** 1709; Chapman W G, Jackson G and Gubbins K E 1988 *Mol. Phys.* **65** 1057
- [3] Chiew Y C 1990 *Mol. Phys.* **70** 129
- [4] Schweitzer K S and Curro J G 1989 *J. Chem. Phys.* **91** 5059
- [5] Dickman R and Hall C K 1988 *J. Chem. Phys.* **89** 3168
- [6] Banaszak M, Chiew Y C and Radosz M 1993 *Phys. Rev.* **E48** 3760; Banaszak M, Chiew Y C and Radosz M 1995 *Fluid Phase Equilibria* **111** 161
- [7] Banaszak M, Chiew Y C, O'Lenick R and Radosz M 1994 *J. Chem. Phys.* **100** 3803
- [8] Yethiraj A and Hall C K 1991 *J. Chem. Phys.* **95** 8484
- [9] Amos M D and Jackson G 1992 *J. Chem. Phys.* **96** 4604
- [10] Malakhov A O and Brun E B 1992 *Macromolecules* **25** 6262
- [11] Sear R P and Jackson G 1994 *Phys. Rev.* **E50** 386
- [12] Mitlin V S and Sanchez I C 1993 *Chem. Phys.* **99** 533
- [13] Huang S H and Radosz M 1990 *Ind. Eng. Chem. Res.* **29** 2284
- [14] Huang S H and Radosz M 1991 *Ind. Eng. Chem. Res.* **30** 1994
- [15] Chen S, Banaszak M and Radosz M 1995 *Macromolecules* **28** 1812
- [16] Chen C K, Banaszak M and Radosz M 1998 *J. Chem. Phys.* **B102** 2427
- [17] Chen C K, Duran M A and Radosz M 1993 *Ind. Eng. Chem. Res.* **32** 3123
- [18] Sheng Y J, Panagiotopoulos A Z, Kumar S T and Szeifer I 1994 *Macromolecules* **27** 400
- [19] Banaszak M, Chen C K and Radosz M 1996 *Macromolecules* **29** 6481
- [20] Eisenberg A and King M 1977 *Ion-Containing Polymers* Academic Press New York
- [21] Gouin J-P, Bosse F, Nguyen D, Williams C E and Eisenberg A 1993 *Macromolecules* **26** 7250
- [22] Banaszak M and Clarke J H R 1999 *Phys. Rev.* **E60** 5753
- [23] Khandpur A K, Forster S, Bates F S, Hamley I W, Ryan A J, Bras W, Almdal K and Mortensen K 1995 *Macromolecules* **28** 8796
- [24] Ryckaert J P, Ciccotti G and Berendsen H J C 1977 *J. Comput. Phys.* **23** 327
- [25] Berendsen H J C, Postma J P M, van Gunsteren W F, Dinola A and Haak J R 1984 *J. Chem. Phys.* **81** 3684
- [26] Banaszak M and Radosz M accepted in *Fluid Phase Equilibria*
- [27] Banaszak M and Clarke J H R submitted for publication

